

Interaction of Electric Fields with Membrane-Bound Polyionic
Proteins

E. Neumann and K. Tsuji

Max-Planck-Institut für Biochemie

D-8033 Martinsried/München FRG

Abstract

Recent progress in electro-optic instrumentation has led to experimental results which give new insight into the dynamic behavior of membrane-bound polyionic macromolecules, such as bacteriorhodopsin in purple membranes. Electric impulses of high field intensity (2×10^5 to 3×10^6 Vm^{-1} , 1 to 20 μs duration) cause transient changes in the optical absorbance of suspended purple membranes of Halobacterium halobium. The electric dichroism at 1 mM NaCl pH \approx 6 and at 293 K is dependent on field strength, pulse duration and wavelength of the monitoring, plane-polarized light in the range 400 nm to 650 nm. The optically indicated processes are, however, independent of bacteriorhodopsin concentration, of ionic strength and of the intensity of the monitoring light. These data and the analysis of time course and steady state of the reduced dichroism suggest electric field sensitive, intramembraneous structural changes which involve restricted orientation changes of the chromophore. A theoretical analysis of restricted orientation is developed and applied to the electro-optic data. As a result it is found that the electric dichroism of purple membranes is associated with a large induced dipole moment up to 7×10^{-26} Cm (2.1×10^4 Debye) which develops in a cooperative manner; the electric permanent dipole moment which is involved amounts to 4.7×10^{-28} Cm (140 Debye).

1. Introduction

Electro-optic and dielectric methods are traditionally applied in order to study not only electrical but also structural properties of dipolar and ionic molecules and molecular organizations. Furthermore, electric field techniques are gaining increasing

importance for the investigation of chemically interacting, ionic or dipolar systems; for review see ref. [1] and [2]. The measurement of electric field effects in biological membranes or biomembrane fragments may, in addition, reveal functionally relevant molecular information, because almost all biomembranes are the locus of strong cross-membrane electric fields and of transient changes in these electric fields. In this context we note that bioelectric signals like the nerve impulse involve transient changes in the electric field of excitable membranes; these electric changes are controlled by local electro-chemical gating processes of as yet largely unknown nature; for review see refs. [3] and [4].

In the following account, a short digression on some fundamental principles of electro-chemical coupling and on the analysis of electrically induced optical changes in chemically interacting systems is given. Using bacteriorhodopsin of purple membranes as an example, basic aspects of the analysis of electro-optic data on membrane-bound proteins are discussed. The results of the theoretical treatment of the experimental data suggest that the orientation changes of the chromophore in bacteriorhodopsin are sterically restricted and are accompanied by a change in the optical extinction coefficient, resulting in a chemical contribution to the absorbance change. For the data analysis an electro-optic theory for restricted orientation is developed. The main result of this study is that external electric fields induce intramolecular structural changes in purple membranes which involve restricted rotation of the chromophore coupled to a very large induced dipole as well as to an electric permanent dipole moment. The order of magnitude of the electric moments points to cooperatively stabilized clusters of bacteriorhodopsin in purple membranes. An electric impulse is able to cause a cyclic change through at least five different conformations of the protein⁵.

The data on bacteriorhodopsin in purple membranes are suggestive of a possibly general mechanism for the interaction of electric fields with membrane-bound proteins, for instance those involved in the electrical-chemical control of ion flows across excitable biomembranes^{3,4}.

2. Primary electric field effects.

The primary effects of electric fields on molecules are fairly well understood: (1) orientation of dipolar species, deformation of polarizable systems (and subsequent orientation of induced dipoles in electrically anisotropic particles); (2) movement of ionic species in the direction of the field vector. Less well explored is how these polarization and electrophoresis effects are specifically coupled to the various chemical transformations, such as conformational transitions or dipolar and ionic association-

dissociation equilibria or steady states. Generally we can only state that polar structures tend to orient in the field direction; conformations or molecules with large dipole moments increase in concentration at the expense of those configurations with smaller electric moments; finally, electric fields increase the dissociation of weak acidic and basic groups and promote the separation of ion pairs into the respective dissociated ions or ionic groups (second Wien effect). For an extended discussion see refs. [1] and [2].

3. Elemental chemical reactions

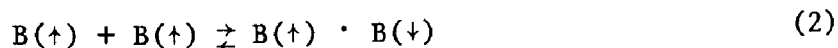
When molecules carrying permanent or induced dipoles or charged groups interact with each other and undergo chemical transformations, three types of electro-chemical coupling may be differentiated: permanent dipole equilibria, induced dipole equilibria, and ionic association-dissociation processes. Changes in the concentration of the reaction partners arise from two types of elemental chemical reactions: inter- and intra-molecular processes.

Intermolecular steps

If the dipole moments of a ligand L and a binding site B are larger than that of the complex LB, then an electric field shifts the equilibrium



to the side of the separated reactions partners. A dimerization equilibrium such as



where the dipole moments of B compensate each other upon complex formation (as indicated by the arrows) is particularly sensitive to an electric field because the electric reaction moment is of the order of the dipole moment of the monomer.

An ionic equilibrium such as



where the association step involves ion pair formation, is usually shifted to the rhs when an electric field is present (dissociation field effect or second Wien effect).

Intramolecular steps

Suppose the molecules B are able to equilibrate between two alternate conformations according to



where B' has a larger dipole moment than B , an electric field will shift the equilibrium toward B' . It is recalled that the equilibrium constant for reaction (4) is defined as $K = [B']/[B]$, where the brackets denote concentration.

4. Thermodynamics of chemical field effects

The equilibrium constant (or the steady-state distribution) constant, K , of a chemical equilibrium is dependent on intensive state variables such as temperature T , pressure P , or an external electric field E . For laboratory conditions the state of zero electric field is generally taken as the reference state; thus at $E = 0$, $K = K_0$. When $K(E)$ is the corresponding value in the presence of an electric field, the condition

$$\Delta K = K(E) - K_0 \ll K_0 \quad (5)$$

specifies a linear approximation, generally valid for the small equilibrium shifts which electric fields can cause.

The isothermal-isobaric displacement of dipolar equilibria in electric fields can be described by a general van't Hoff relationship:

$$\left(\frac{\partial \ln K}{\partial E} \right)_{P,T} = \frac{\Delta M}{RT} \quad (6)$$

where R is the gas constant and ΔM is the electric reaction moment defined by

$$\Delta M = N_A \left\{ \sum_j \nu_j \alpha_j (E_i)_j + \sum_j \nu_j p_j \cdot L(r_j) \right\} \quad (7)$$

In Eq. (7), N_A is the Avogadro number; ν_j is the stoichiometric coefficient (counting positive for products and negative for reactants), α_j is the electric polarizability, p_j is the permanent dipole moment^j of species j ; E_i is the internal field and $L(r_j)$ is the Langevin function of the ratio $r_j = p_j E_d / kT$, E_d being the directing field.

In the range where Eq. (5) is applicable, integration of Eq. (6) provides an expression for the field-induced shift in K :

$$\frac{\Delta K}{K_0} = \frac{1}{RT} \int \Delta M dE \quad (8)$$

Ionic equilibria can be treated in an analogous way, see, e.g., refs [1] and [2].

The general relationship in Eq. (8) can be further specified. For instance, if pure induced dipoles interact, Eqs. (7) and (8) yield:

$$\frac{\Delta K}{K_0} = \frac{1}{kT} \int \sum v_j \alpha_j (E_i)_j dE \quad (9)$$

At field strengths which saturate the induced dipole moments $m_j = \alpha_j (E_i)_j$ to $(m_j)_s$, the system behaves like a permanent dipole equilibrium and

$$\frac{\Delta K}{K_0} \approx \frac{f(\epsilon, n)}{6(kT)^2} \sum v_j (m_j)_s^2 \cdot E^2 \quad (10)$$

where $f(\epsilon, n)$ is a function of the dielectric constant and the refractive index of the solvent and where we assume that $(E_i)_j = E_i = f(\epsilon, n) \cdot E$; see refs. [1] and [2].

For the intramolecular step of Eq. (4) we have $v_{B'} = 1$, $v_B = -1$; with the assumption that $(E_i)_{B'} = (E_i)_B = E_i = f(\epsilon, n) \cdot E$ we obtain $M_{B'} = N_A \cdot \alpha_{B'} \cdot E_i$, $M_B = N_A \cdot \alpha_B \cdot E_i$. Then, $\Delta M = M_{B'} - M_B = N_A \cdot \Delta \alpha \cdot E_i$ where $\Delta \alpha = \alpha_{B'} - \alpha_B$, and

$$\frac{\Delta K}{K_0} = \frac{f(\epsilon, n)}{kT} \int \Delta \alpha \cdot E dE \quad (11)$$

Provided that $\Delta \alpha$ is constant, i.e. at small field strengths,

$$\frac{\Delta K}{K_0} \approx \frac{f(\epsilon, n)}{2kT} \Delta \alpha \cdot E^2 \quad (12)$$

and at saturating field intensities,

$$\frac{\Delta K}{K_0} \approx \frac{f(\epsilon, n)}{6(kT)^2} (\Delta m)_s \cdot E^2 \quad (13)$$

where $(\Delta m)_s = (m_{B'})_s - (m_B)_s$. As seen in Eqs. (12) and (13) an induced dipole mechanism is characterized by a temperature variation from T^{-2} to T^{-1} . It should be mentioned that there are several experimentally useful criteria to differentiate the various mechanisms and types of electric interactions [1,2].

The concentration changes described by ΔK may be indicated by optical and/or electrical methods; variations with T and E may then be used to identify type and mechanism of interaction.

Experimentally, recent progress in instrumentation has opened the way for measuring field-induced, rotational and chemical relaxations in parallel, both optically and electrically, even in the nanosecond time range^[6]. It is obvious that the analysis of the kinetics and thermodynamics of these relaxations is particularly straightforward when rectangular pulses are applied.

5. Rotational and chemical contributions to absorbance changes

The absorbance per cm of a multi-component system is generally given by Lambert-Beer's law:

$$A = \sum_i \epsilon_i c_i \quad (14)$$

where ϵ_i is the molar extinction coefficient and c_i is the molar concentration of species i . It is recalled that the extinction coefficients of molecules which are intrinsically optically anisotropic, reflect average values $\bar{\epsilon}_i$ of all chromophore orientations in the system.

In principle both the ϵ_i and c_i -terms may be field dependent such that in general,

$$dA = \sum_i c_i \left(\frac{\partial \epsilon_i}{\partial E} \right)_{c_i} dE + \sum_i \epsilon_i \left(\frac{\partial c_i}{\partial E} \right)_{\epsilon_i} dE \quad (15)$$

More specifically, when an electric field is applied to a chemical system which exhibits both electrical and optical anisotropy, the field induced absorbance change ΔA_σ , measured with light polarized at angle σ relative to the electric _{σ} field vector, may not only involve orientational changes ($\Delta \epsilon_{i,\sigma}$) but also concentration changes (Δc_i).

In the absence of an electric field the absorbance per cm of such a system is expressed by

$$A = \sum_i \bar{\epsilon}_i c_i^0 \quad (16)$$

Whereas A is independent of σ , the absorbance in the field is σ -dependent:

$$A_\sigma^E = \sum_i \epsilon_{i,\sigma}^E c_i^E \quad (17)$$

Denoting the field induced changes in ϵ_i and c_i by

$$\begin{aligned} \Delta \epsilon_{i,\sigma} &= \epsilon_{i,\sigma}^E - \bar{\epsilon}_i \\ \Delta c_i &= c_i^E - c_i^0 \end{aligned} \quad (18)$$

the field-induced absorbance change $\Delta A_{\sigma} = A_{\sigma}^E - A$ is rewritten in terms of Eqs. (16) and (17):

$$\begin{aligned} \Delta A_{\sigma} &= \sum_i (\epsilon_{i,\sigma} c_i^E - \bar{\epsilon}_i c_i^0) \\ &= \sum_i \Delta \epsilon_{i,\sigma} (c_i^0 + \Delta c_i) + \sum_i \bar{\epsilon}_i \Delta c_i, \end{aligned} \quad (19)$$

where the separation of terms depending on σ from those independent of σ is apparent. Introducing the definitions

$$\Delta A_{\sigma}^{(\text{rot})} = \sum_i \Delta \epsilon_{i,\sigma} (c_i^0 + \Delta c_i) \quad (20)$$

and

$$\Delta A^{(\text{chem})} = \sum_i \bar{\epsilon}_i \Delta c_i, \quad (21)$$

Eq. (19) may be generally written in terms of a rotational and a chemical contribution [7]:

$$\Delta A_{\sigma} = \Delta A_{\sigma}^{(\text{rot})} + \Delta A^{(\text{chem})} \quad (22)$$

For axially symmetric systems $\Delta A^{(\text{chem})}$ can be experimentally obtained in two independent ways, using the measured absorbance changes ΔA_{σ} at the polarization modes $\sigma=0$ and $\sigma=\pi/2$, or $\sigma=0.955$ rad (54.7°). In this case the relationship

$$\Delta A_{||}^{(\text{rot})} + 2\Delta A_{\perp}^{(\text{rot})} = 0 \quad (23)$$

holds, and for $\sigma=0.955$ rad Eq. (22) reduces to

$$\Delta A_{0.955} = \Delta A^{(\text{chem})} \quad (24)$$

On the other hand, Eqs. (22) and (23) can be combined to yield

$$\frac{1}{3} (\Delta A_{||} + 2 \Delta A_{\perp}) = \Delta A^{(\text{chem})} \quad (25)$$

Therefore, the equality

$$\Delta A_{0.955} = \frac{1}{3} (\Delta A_{||} + 2\Delta A_{\perp}) \quad (26)$$

can be used as a criterion for axial symmetry of the electric dipole moment of the orienting unit.

Note that $\Delta A^{(\text{rot})}$ specified in Eq. (20) may contain concentration changes Δc_i^{σ} . These changes ($\sum \Delta \epsilon_{i,\sigma} c_i^{\sigma}$), are separable from the pure rotational term $\sum \Delta \epsilon_{i,\sigma} c_i^0$, only when the kinetics of the rotational part is faster than the concentration changes [1, 2].

6. Conformational changes induced by electric fields in bacteriorhodopsin

Bacteriorhodopsin is the photoactive protein of the purple membrane which is a specialized part of the cell membrane of many halobacteria⁸. The protein functions as a light-driven proton pump producing an electrochemical proton gradient from which finally the free energy of the light induced ATP synthesis is derived⁹. As an integral membrane protein, bacteriorhodopsin is exposed to the internal electric field of the membrane. In order to study the structural and functional effects of the intrinsic electric field and of variations of the membrane field, isolated purple membrane fragments may be subjected to external electric impulses. Provided that electric-field induced structural changes are accompanied by variations in the chromophore and its protein environment, specified conformational transitions should be optically measurable. Light transmission changes have been indeed observed when field pulses were applied to purple membranes¹⁰⁻¹³ as well as to apomembrane fragments¹¹. However, type and mechanism of the optical signal changes have not been analyzed.

Orientation of whole membrane fragments will contribute to the optical signal if the applied electric fields last longer^{10,12,14}. In rectangular electric pulses of short duration the contribution of fragment orientation is negligibly small and does not interfere with electro-optical signals arising from intramembraneous processes.

6.1 Theory of restricted orientation

The experimental data indicate that bacteriorhodopsin in purple membranes are electro-optically anisotropic. The chromophore is a part of a rather rigid protein-lipid structure¹⁵, hence orientational displacements of the chromophore within the protein are expected to be sterically restricted. Limited orientation is different from rotations of freely mobile particles and requires a different theoretical analysis⁵.

It is known that the angle ψ between the chromophore transition moment μ of bacteriorhodopsin and the membrane normal is about 1.2 rad (70°)¹⁶⁻¹⁸. The electro-optic data of the present study suggest that an electric field E causes an angular displacement $\Delta\psi$ of μ from the position ψ^0 in the absence of a field. As exemplified in Figure 1(a), steric restriction may cause, for instance, that $\Delta\psi$ is limited to a maximum value $\Delta\psi_m$. Generally two limiting cases of orientational restriction may be considered for the membrane bound proteins, when the membrane fragments themselves remain distributed randomly.

In Case I, μ may be displaceable in both directions relative

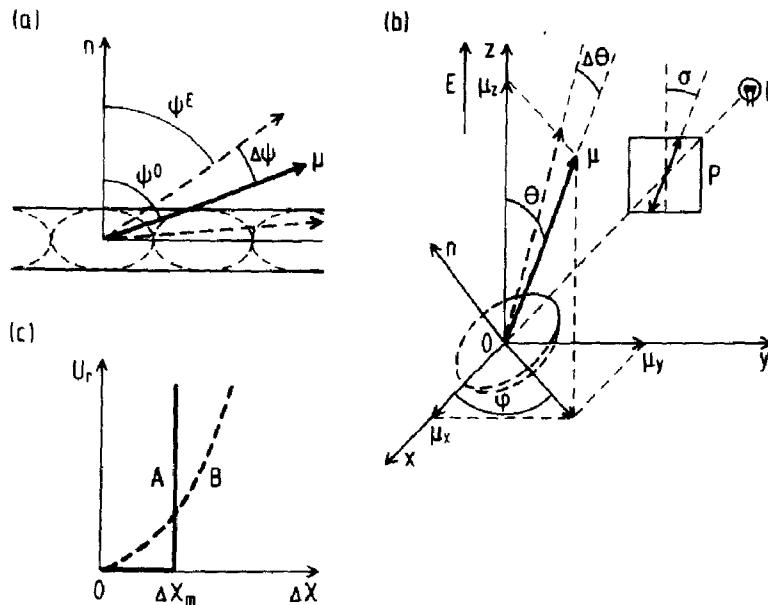


Fig. 1 (a) Cross section of purple membrane; parallel to the membrane normal n ; μ , optical transition moment; $\Delta\psi$ is the angular displacement in an electric field E . Case I: μ can rotate symmetrically toward and away from n such that $\psi^E = \psi^0 \pm \Delta\psi$. Case II: μ can rotate to only one side, e.g., $\psi^E = \psi^0 - \Delta\psi$ leading to positive dichroism.

(b) Geometrical relations of electric dichroism in Cartesian coordinates. E is in the z -direction, the light beam from a source L is in the x -axis and the polarizer, P , is in the y, z -plane providing plane-polarized light under the angle σ relative to E . The optical transition moment μ of a particular chromophore lies under the angle θ to E .

(c) Dependence of the restriction energy term U_r on the angular displacement $\Delta\chi$ for Model A (well-type potential energy profile) and Model B (potential energy according to Hooke's Law).

to the membrane normal, either increasing or decreasing ψ . Hence, this angular displacement is symmetric and, in the field, we obtain $\psi^E = \psi^0 \pm \Delta\psi$.

In Case II, μ can rotate in only one direction. This asymmetric displacement leads to $\psi^E = \psi^0 - \Delta\psi$ for positive dichroism and, alternatively, to $\psi^E = \psi^0 + \Delta\psi$ for negative dichroism. If Case II applies, only one half of the membrane fragments are affected by the electric field.

Orientation factor

The formalism to calculate the orientation factor for restricted orientation is analogous to that for free, unrestricted orientation. Therefore, the key equations for free orientation¹⁹ are given first.

The absorbance change, ΔA_σ , caused by the electric field, E , in an electro-optically anisotropic system, measured with light that is plane-polarized at the angle σ with respect to E (see Figure 1(b)), is given by $\Delta A_\sigma = A_\sigma^E - A$ where A_σ^E is the absorbance in the presence of the field and A is the absorbance at $E = 0$.

The reduced absorbance change is generally expressed in terms of the orientation factor Φ according to

$$\frac{\Delta A_\sigma}{A} = \frac{1}{2}(3\cos^2\omega - 1)(3\cos^2\sigma - 1)\Phi \quad (27)$$

where ω is the fixed angle between the optical transition moment μ and the electrical symmetry axis of the orienting unit (permanent and induced dipoles)²⁰.

The reduced dichroism is defined by

$$\frac{\Delta A}{A} = \frac{A_{||}^E - A_{\perp}^E}{A} = \frac{3}{2}(3\cos^2\omega - 1)\Phi \quad (28)$$

where $A_{||}^E$ and A_{\perp}^E are the absorbance values measured in the parallel ($\sigma=0$) and in the perpendicular ($\sigma=\pi/2$) modes of light polarization, respectively.

The orientation factor is given by

$$\Phi = \frac{1}{2}(3\langle\cos^2\chi\rangle - 1) \quad (29)$$

where χ is the angle between the electric symmetry axis of the orienting unit and the direction of the external electric field.

The average value of $\cos^2 \chi$ is defined by

$$\langle \cos^2 \chi \rangle = \int_0^\pi \cos^2 \chi f_\chi 2\pi \sin \chi d\chi \quad (30)$$

and the angular distribution function of the orienting unit for the steady state is given by

$$f_\chi = \frac{\exp(-U/kT)}{\int_0^\pi \exp(-U/kT) 2\pi \sin \chi d\chi} \quad (31)$$

where k is the Boltzmann constant and T is the absolute temperature.

The potential energy, U , of a freely orienting unit characterized by the permanent dipole moment p and by the excess polarizabilities α_1 (parallel to the electric symmetry axis) and α_2 (perpendicular to it) is given by

$$U = -pE_d \cos \chi - \frac{1}{2}(\alpha_1 - \alpha_2)E_i^2 \cos^2 \chi \quad (32)$$

where, to a first approximation, we assume that the directing field E_d and the internal field E_i are equal to the external field E ; see discussion. Introducing Eqs. (30) to (32) into Eq. (29) yields the familiar relationship

$$\Phi = \frac{3 \int_{-1}^1 u^2 \exp(\beta u + \gamma u^2) du}{2 \int_{-1}^1 \exp(\beta u + \gamma u^2) du} - \frac{1}{2} \quad (33)$$

where

$$u = \cos \chi$$

$$\beta = pE_d/kT$$

$$\gamma = (\alpha_1 - \alpha_2)E_i^2/(2kT).$$

For restricted orientation the potential energy may be written in two terms:

$$U = U_o + U_r \quad (34)$$

where U_o has the form of Eq. (32) and the restriction term U_r specifies the type of steric restriction. Obviously, for unrestricted, free orientation, $U_r = 0$ and $U = U_o$. In general, with respect to χ , orientation is viewed as an angular displacement $\Delta \chi$ of the electric symmetry axis of the orienting unit from a position χ^o at $E = 0$ to a position χ^E in the presence of the field; hence

$\Delta\chi = \chi^0 - \chi^E \geq 0$. Whereas in unrestricted, free orientation $\Delta\chi$ does not enter into the energy term, restricted orientation may be explicitly expressed as a function of $\Delta\chi$. The further analysis in this study will be confined to the theoretical treatment of two physically simple models.

In Model A the steric restriction is approximated by a well-type energy profile for U_r with infinitely high boundaries. The angular displacement is therefore subjected to the condition $0 \leq \Delta\chi \leq \Delta\chi_m$ where $\Delta\chi_m$ is the maximum displacement which corresponds to a maximum $\Delta\psi_m$ for the displacement of the chromophore μ relative to the membrane normal; see Figure 1(a). The restriction term U_r is then $U_r = 0$ for $0 \leq \Delta\chi \leq \Delta\chi_m$, and $U_r = \infty$ for $\Delta\chi > \Delta\chi_m$, and the total energy is given by:

$$U = -pE \cos \chi^E - \frac{1}{2}(\alpha_1 - \alpha_2)E^2 \cos^2 \chi^E, \text{ for } (\chi^0 - \Delta\chi_m) \leq \chi^E \leq (\chi^0 + \Delta\chi_m) \quad (35)$$

$$U = \infty, \text{ for } 0 \leq \chi^E < (\chi^0 - \Delta\chi_m) \text{ or } \chi^E > (\chi^0 + \Delta\chi_m)$$

The potential energy is a function of two variables χ^0 ($0 \leq \chi^0 \leq \pi$) and χ^E ($0 \leq \chi^E \leq \chi^0$); note that χ^0 is independent of χ^E . Therefore we may introduce a partial orientation factor ϕ_{χ^0} for the particular angular position χ^0 . Then, the orientation factor ϕ can be obtained as the average of ϕ_{χ^0} for all angular directions χ^0 :

$$\phi = \frac{1}{2} \int_0^\pi \phi_{\chi^0} \sin \chi^0 d\chi^0 \quad (36)$$

Note that the integral is reduced by a factor 1/2 in Case II because for one half of the system there is no orientation.

The partial orientation factor is now obtained from Eqs. (29) to (33) with $\chi = \chi^E$. For the Model A Eq. (35) is introduced into Eq. (31), respectively. The respective partial orientation factor is then:

$$\phi_{\chi^0} = \frac{3 \int_{u_1}^{u_2} u^2 \exp(\beta u + \gamma u^2) du}{2 \int_{u_1}^{u_2} \exp(\beta u + \gamma u^2) du} - \frac{1}{2} \quad (37)$$

with $u_1 = \cos(\chi^0 + \Delta\chi_m)$ and $u_2 = \cos(\chi^0 - \Delta\chi_m)$.

For the analytical treatment of model B see ref. [5].

The results of numerical calculations of Eq. (36) for the symmetric Case I and the asymmetric Case II are shown in Figure 2, using Model A (well-type energy profile) with $\Delta\chi_m$ as a parameter and Model B (Hooke-type energy profile) with a/kT as a parameter, respectively.⁵ Note that the variable $(\beta^2 + 2\gamma)$ with the permanent (β) and the induced (γ) dipole terms defined by Eq. (33) is proportional to E^2 . Therefore the field strength dependence of the reduced dichroism can be curvefitted to the function $\Phi(\beta^2 + 2\gamma)$. Hence, the mechanism as well as the type of orientation (free or restricted) may be determined.

Electric dichroism of restricted orientation. The primary data of electric dichroism of systems like purple membranes are related to the angle θ between the optical transition moment μ of a particular chromophore (or clusters of chromophores) and the direction of the external electric field; see Figure 1(b). For the sake of simplicity we shall at first assume that the electric symmetry axis is parallel to the optical transition moment ($\omega=0$). This assumption is in line with the observation of positive dichroism; see Eq. (28). Furthermore, as demonstrated below the experimental data on membrane-bound bacteriorhodopsin can be consistently analyzed in terms of an axially symmetric overall electric moment. For $\omega=0$, the boundary conditions for θ are the same as those for χ discussed in the previous section.

For Model A the further treatment is particularly simple if the saturation value Φ_s of the orientation factor is considered. At sufficiently high external electric fields all chromophore transition moments which have orientations between $\theta^0 = 0$ and $\theta^0 = \Delta\theta_m$ are parallel to E, i.e., $\theta^E = 0$. The remaining molecules whose transition moments are positioned between $\theta^0 = \Delta\theta_m$ and $\theta^0 = \pi$ assume the positions $\theta^E = \theta - \Delta\theta_m$ for the permanent dipole orientation; while $\theta^E = \theta^0 - \Delta\theta_m$ when $\Delta\theta_m \leq \theta^0 \leq \pi/2$ and $\theta^E = \theta^0 + \Delta\theta_m$ when $\pi/2 \leq \theta^0 \leq \pi - \Delta\theta_m$ for the induced dipole orientation.

The reduced absorbance changes, $\Delta A_\sigma/A$, for maximum angular displacement of the chromophore are readily obtained. For Case I the saturation values are:

(i) permanent-dipole orientation

$$\left(\frac{\Delta A_\sigma}{A}\right)_s = \frac{1}{4}(3 - 2\cos\Delta\theta_m - \cos^2\Delta\theta_m)(3\cos^2\sigma - 1) \quad (38)$$

(ii) induced-dipole orientation

$$\left(\frac{\Delta A_\sigma}{A}\right)_s = (1 - \cos\Delta\theta_m + \sin\Delta\theta_m \cos\Delta\theta_m)(3\cos^2\sigma - 1). \quad (39)$$

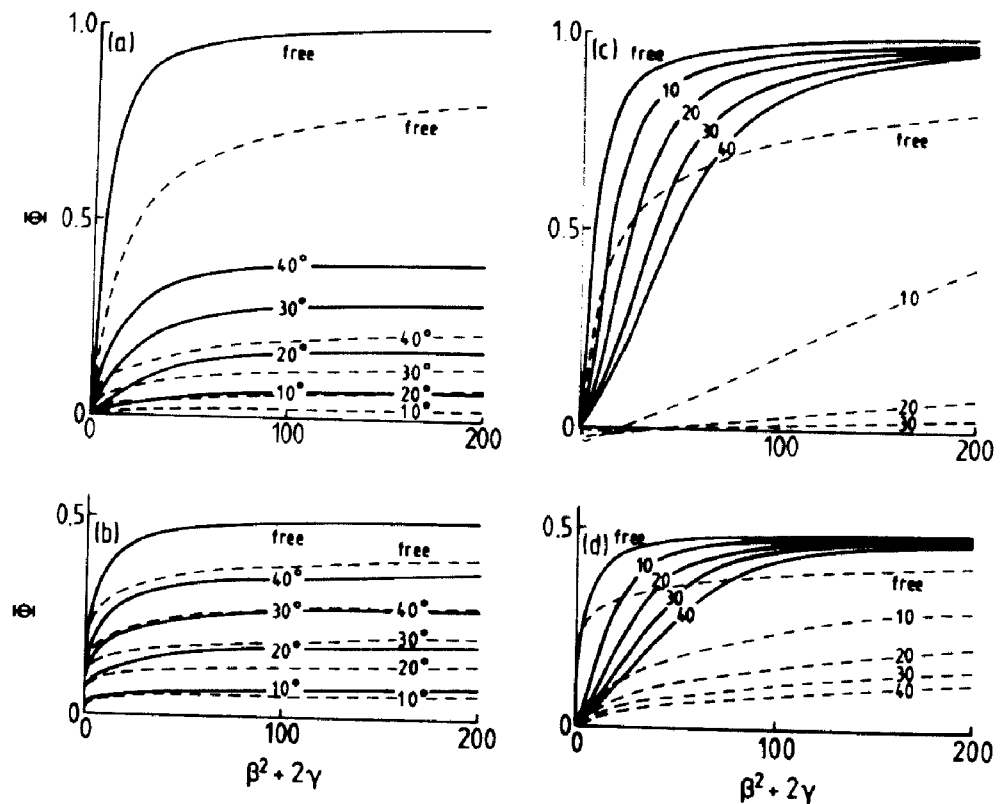


Fig. 2: Orientation factor ϕ for restricted angular displacements $\Delta\chi_m$ of the electric axis as a function of $\beta^2 + 2\gamma$; for comparison, unrestricted free orientation is included. --- refers to ϕ due to pure permanent dipoles, i.e., $\gamma = 0$; ——— refers to ϕ due to induced dipoles, i.e., $\beta = 0, \gamma > 0$.

The parts (a) and (b) refer to Cases I and II, respectively, assuming the restriction energy Model A for various maximum angular displacements $\Delta\chi_m$ as a parameter. Parts (c) and (d) refer to Cases I and II, respectively, assuming the restriction energy Model B for various values of a/kT .

These relationships permit an experimental determination of $\Delta\theta_m$. It should be mentioned that the assumption of $\omega=0$, involved in the derivation of Eqs. (38) and (39), provides a minimum estimate for $\Delta\theta_m$. For this case, $\Delta\theta_m = \Delta\chi_m = \Delta\psi_m$, and the maximum angular displacement relative to the membrane normal is obtained.

6.2 Experimental

The concentration of bacteriorhodopsin in purple membranes isolated from the M1 strain of Halobacterium halobium was determined on the basis of the extinction coefficient $\epsilon = 63000 \text{ M}^{-1}\text{cm}^{-1}$ at 570 nm^{14} .

The optical density of purple membrane suspension for the electric pulse measurements was adjusted to about 0.3 in 1 mM NaCl solution at 293 K, unbuffered (pH \sim 6), unless otherwise stated. The optical density value of 0.3 corresponds to a concentration which yields sufficiently large signals without serious light scattering contributions by the membrane fragments. The electro-optic measurements were performed with an electric-field-jump apparatus recently developed by Schallreuter, Rohner and Neumann⁶. Rectangular electric pulses up to 35 kV and of various durations between 1 μs and 100 μs were used. All measurements were carried out at 293 K. The temperature increase due to Joule heating can be calculated. For the highest voltage $V = 35\text{kV}$ and the longest pulse duration of $\Delta t = 100 \mu\text{s}$, the temperature increase $\Delta T = 3.5 \text{ K}$ is negligibly small, because the absorbance change from 293 K to 296.5 K is less than 3%.⁵

The change in the absorbance ΔA_σ , defined above is calculated from the light transmittance at a given wavelength and a fixed light polarization mode σ :

$$\Delta A_\sigma = -\log(1 + \Delta I_\sigma/I)$$

where I is the transmitted light in the absence of the electric field (independent of σ). The field induced transmittance change is given by $\Delta I_\sigma = I_\sigma^E - I$ where I_σ^E is the light transmitted in the presence of the electric field. It is noted that in this study ΔI_σ is generally not small compared to I . Therefore, the approximation $\Delta A_\sigma = -0.4343\Delta I_\sigma/I$ cannot be applied.

6.3 Results

In Figure 3 typical signal changes induced by an electric impulse in purple membrane suspensions at two light polarization modes are shown. At an electric field strength of $E = 15.4 \times 10^5 \text{ Vm}^{-1}$ a time independent, steady-state level of the light transmittance in the field (subscript ss) is reached only if the pulse duration is equal to or larger than 6 μs . For the parallel ($\sigma=0$)

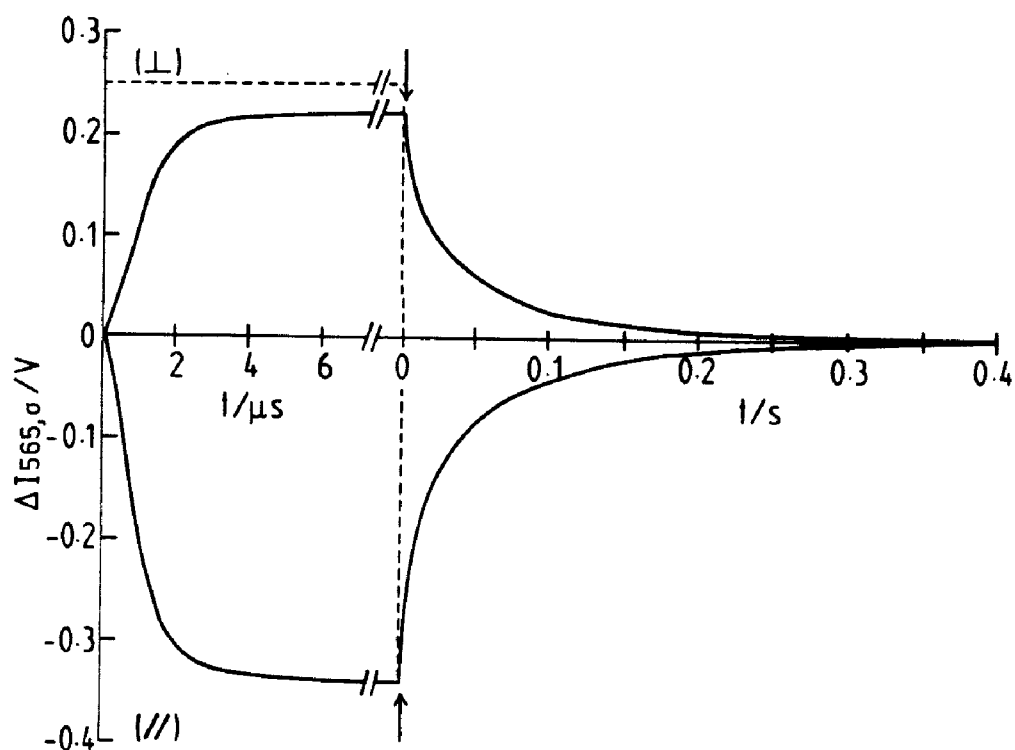


Figure 3: Electric dichroism of bacteriorhodopsin in purple membrane; concentration of bacteriorhodopsin $c = 4.8 \times 10^{-6}$ M in 1 mM NaCl, unbuffered, $\text{pH} \approx 6$, $T = 293$ K. The light transmittance change ΔI_{σ} at $\lambda = 565$ nm is caused by a rectangular electric pulse of $E = 15.4 \times 10^5$ Vm^{-1} applied at $t=0$ for $20 \mu\text{s}$ (see arrows). (//) and (\perp) are the signal changes for light plane-polarized parallel ($\sigma=0$) and perpendicular ($\sigma=\pi/2$) to the electric field; the light intensity I at $t=0$ is 3.0 V.

and the perpendicular ($\sigma=\pi/2$) polarization modes of the monitoring light the reduced absorbance changes calculated according to Eq. (27) are $(\Delta A_{\parallel}/A)_{ss} = 0.32 \pm 0.02$ and $(\Delta A_{\perp}/A)_{ss} = -0.27 \pm 0.02$.

As seen in Figure 3, the signal change, after the electric field is switched off, reflects a continuous relaxation spectrum. At the present accuracy of data recording, the corresponding absorbance curves may be formally described in terms of at least four exponential components according to

$$\frac{\Delta A(t)}{\Delta A_{ss}} = \sum_{i=1}^n \delta_i \exp(-t/\tau_i) \quad (n \geq 4)$$

where ΔA_{ss} is the steady-state absorbance change (when the pulse is terminated) and δ_i and τ_i are the relative amplitude and relaxation time of component i , respectively. For the curve in Figure 3 it is found that $\tau_1 = 0.3 \pm 0.03$ ms, $\tau_2 = 3.0 \pm 0.3$ ms, $\tau_3 = 26 \pm 4$ ms, $\tau_4 = 100 \pm 10$ ms; $\delta_1 \approx 0.2$, $\delta_2 \approx 0.2$, $\delta_3 \approx 0.3$, $\delta_4 \approx 0.3$.

Compared to the time range of the rise curve in the presence of the electric field, the field-off response is slower by orders of magnitude. This experimental result already indicates that the optical data cannot reflect simple, free orientation of the chromophore.

Figure 4 shows the field strength dependence of the reduced absorbance change (steady-state) at $\lambda = 565$ nm for three light polarization modes; $\sigma=0$, parallel; $\sigma=\pi/2$, perpendicular; $\sigma=0.955$ rad (54.7°). Note that the absorbance change ΔA_{\parallel} apparently saturates at $E > 4 \times 10^5$ Vm $^{-1}$ while $-\Delta A_{\perp}$ still increases with increasing field strength.

It is found that the reduced absorbance change (steady-state) depends on the wavelength of the monitoring light, in a different manner for the various polarization modes. In particular, the parallel mode has a pronounced maximum at about 565 nm. The ratio of the absorbance changes, $(\Delta A_{\parallel}/\Delta A_{\perp})$, equals -1.2 ± 0.2 at 565 nm; at 400 nm this ratio is -0.5 ± 0.05 . The value of $\Delta A_{0.955}/A$ is larger at 400 nm than at 565 nm. The reduced absorbance changes (steady state) at $\sigma=0$ and $\sigma=\pi/2$ are found to be independent of purple membrane concentration between 1.4×10^{-6} M and 2.0×10^{-5} M and of ionic strength between 1 mM and 3 mM NaCl. The intensity of the monitoring light affects only very slightly the magnitude of the reduced absorbance changes. Thus light induced contributions to ΔA_{σ} are negligibly small.

The relaxation times of the field-off responses are, within

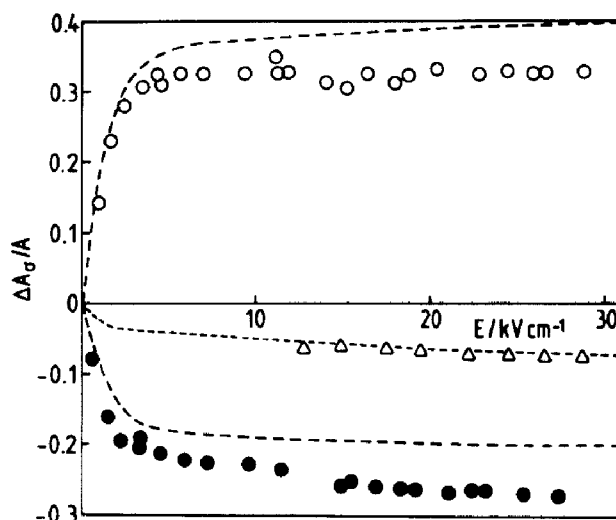


Fig. 4: The electric field strength dependence of the steady-state value of the reduced absorbance change $\Delta A_{\sigma}/A$ for the purple membrane suspension at $\lambda = 565$ nm: \circ , $\sigma=0$; \bullet , $\sigma = \pi/2$, and Δ , $\sigma = 0.955$. The dashed curves were calculated according to equation (40): --- refers to $\Delta A_{\sigma}^{(rot)}/A$ at $\sigma=0$ and $\sigma=\pi/2$; --- refers to $\Delta A^{(chem)}/A$. The other experimental conditions are the same as in Figure 3.

experimental error, independent of the field strength, pulse duration, wavelength, light polarization direction, concentration of purple membrane, ionic strength and the intensity of the monitoring light.

6.4 Discussion

The primary experimental data, ΔA_{σ} , on purple membranes do not follow Eq. (23), i.e., $\Delta A_{\parallel} + 2\Delta A_{\perp} \neq 0$. Therefore, chemical changes may be involved. If, however, $\Delta A_{0.955}$ is compared with $(\Delta A_{\parallel} + 2\Delta A_{\perp})/3$, it is found that Eq. (26) holds. Hence, the system exhibits axial symmetry and Eq. (22) in the form

$$\Delta A_{\sigma}^{(rot)} = \Delta A_{\sigma} - \Delta A_{0.955} \quad (40)$$

can be used to calculate the rotational contributions of ΔA_{σ} . The experimental data represented in Figure 4 are evaluated according to this subtraction procedure and the results are included as dashed lines.

The wavelength dependence of $\Delta A_{\sigma}^{(rot)}/A$ suggests that the absorption band between 400 nm and 650 nm arises from at least two different optical transitions. It is noted, too, that the chemical contribution ($\Delta A_{0.955}/A$) is larger at 400 nm (-0.14 ± 0.02) than at 565 nm (-0.055 ± 0.005). It is seen in Figure 4 that the reduced changes in $\Delta A_{\parallel}^{(rot)}/A$ and $-\Delta A_{\perp}^{(rot)}/A$ increase with

increasing field strength in qualitatively the same way as $\Delta A^{(\text{chem})}/A$.

The practical coincidence of $\Delta A_{\text{O}}^{(\text{rot})}$ with $\Delta A^{(\text{chem})}$ is not only reflected in the steady-state but also in the kinetics; the entire time courses of the relative signal changes in the various polarization modes, i.e., the rotational and the chemical contributions, are coincident within the margin of experimental error. These results suggest that $\Delta A^{(\text{chem})}$ and $\Delta A_{\text{O}}^{(\text{rot})}$ reflect two aspects of one and the same process which is induced by the electric field.

Orienting unit. As is described above, the reduced absorbance changes are independent of bacteriorhodopsin concentration and of the ionic strength of the suspension. Therefore, particle-particle interactions may be considered as negligibly small.

Electric dichroism may be caused by orientation of entire membrane fragments. Purple membrane fragments are oriented by long lasting, exponentially decaying electric fields^{10,12}, or in relatively low electric field strengths ($1 \times 10^4 \text{ Vm}^{-1}$) applied for a sufficiently long time (1-2 min)¹⁴. The time constant for fragment orientation can be estimated using Perrin's equation²¹. Purple membranes may be considered as oblate discs with diameters between 0.5 μm and 1 μm ²²; the rotational time constants for these dimensions are in the order of 100 ms.

It was recently shown that electric fields of low intensity and a duration of several seconds orient purple membrane fragments. The dichroism of fragment orientation is, however, negative and suggests orientation of the membrane normal parallel to E.²³

The positive dichroism observed in our study with short-lasting high field intensity pulses can therefore not come from fragment orientation. In addition, pure fragment orientation is not expected to result in a chemical contribution to the absorbance changes.

A further possibility for orientational changes is the bending of membrane fragments. Because purple membranes are known to be rather rigid protein lipid lattices¹⁵, it is improbable that the optical signals are caused by fragment bending.

We are thus driven to conclude that the bacteriorhodopsin molecules themselves are the origin of the observed electric dichroism. The rigidity of the hexagonal lattice would, however, prevent the protein molecule from changing position as a whole within the membrane²⁴. It is more likely that only local parts of the protein involving the chromophore can move to a limited extent in the electric field; restricted chromophore motion is also apparent in the light-induced photocycle^{11,25-30}.

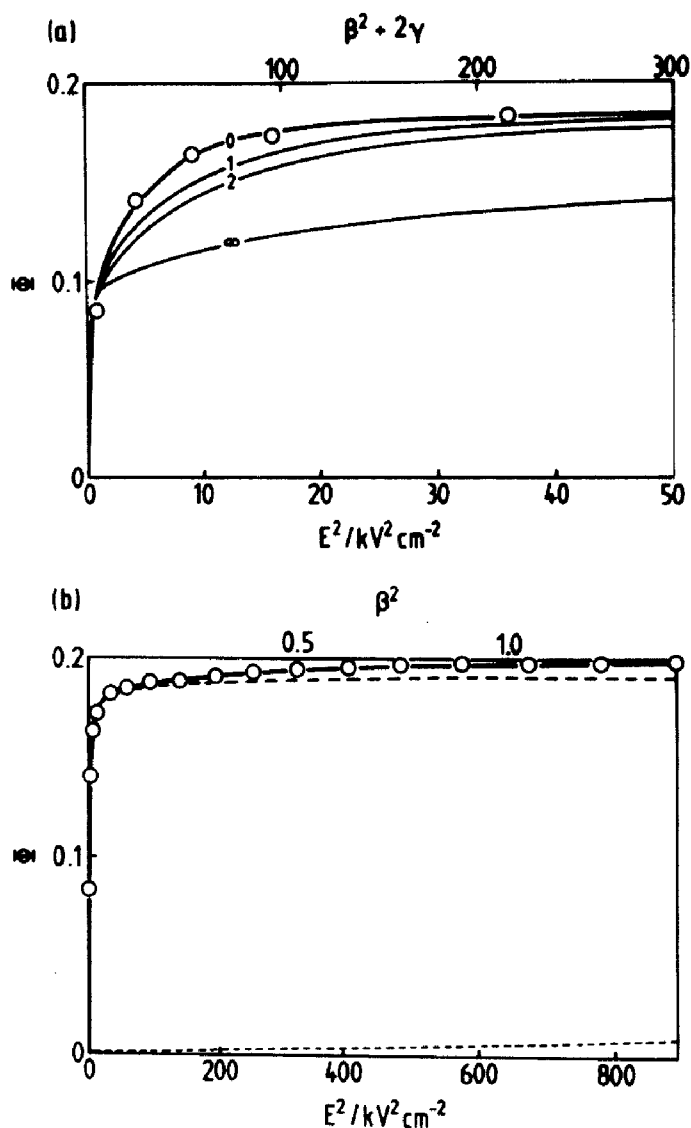


Figure 5: Electric field strength dependence of the orientation factor ϕ in terms of E^2 , $\beta^2+2\gamma$ and β^2 , for restricted angular displacement of the electric dipole axis from χ^0 to $\chi^0-\Delta\chi_m$; $\Delta\chi_m = 0.35$ rad (20°). (a) Low field strength range for various ratios of $\beta^2/2\gamma$ (—). (b) Total experimental range of E : — — — refers to the induced dipole contribution (2γ); ---- refers to the permanent dipole contributions. The comparison with the experimental data (O) involves the assumption that $\omega=0$.

In summary, the electro-optic signals described in this study most probably result from electric-field-induced structural changes which can be identified as limited orientational changes involving the chromophore.

Orientation mechanism. Applying the theory for restricted orientation to the field strength dependence of the reduced dichroism $\Delta A^{(\text{rot})}/A$, we obtain the mechanism for the angular displacement of the chromophore in bacteriorhodopsin. According to Eqs. (28) and (33), the orientation factor ϕ is proportional to $\Delta A^{(\text{rot})}/A$ and $|\beta^2 + 2\gamma|$ is proportional to E^2 , respectively. Therefore, the experimental data set $\Delta A^{(\text{rot})}/A$ is fitted to the theoretical curves of ϕ versus $|\beta^2 + 2\gamma|$ (see Figure 2), using proper scale factors³¹. It is found that among the models considered, only Case II of Model A gives satisfactory results; Case I(A) and Model B as well as free orientation can be excluded.

According to the observation of positive dichroism we assume for simplicity that ($\omega=0$). In detail, Figure 5(a) shows the comparison of ϕ from $\Delta A^{(\text{rot})}/A$ (steady-state) with ϕ calculated for Case II(A) with $\Delta\chi_m = 0.35$ rad as a function of $\beta^2 + 2\gamma$ for various ratios of $\beta^2/2\gamma$; ($\gamma>0$). The experimental data fit the curve for $\beta^2/2\gamma = 0$ up to $E^2 = 5 \times 10^{11} \text{ V}^2\text{m}^{-2}$, if at $E^2 = 1 \times 10^{11} \text{ V}^2\text{m}^{-2}$, $\beta^2 + 2\gamma = 60$ and if $\phi = 0.19$ for $\Delta A^{(\text{rot})}/A = 0.57$. The low field strength range is thus dominantly determined by an induced dipole moment.

An additional slight increase in ϕ becomes apparent at higher field strengths ($E^2 > 5 \times 10^{11} \text{ V}^2\text{m}^{-2}$) and can be attributed to a permanent dipole moment.

Figure 5(b) summarizes the results: the entire experimental field strength range is quantitatively described by the maximum angular displacement $\Delta\chi_m = 0.35$ rad, the permanent dipole moment $p = 4.7 \times 10^{-28} \text{ Cm}$ (140 Debye) and the excess polarizability difference $\alpha_1 - \alpha_2 = 2.4 \times 10^{-30} \text{ Fm}^2$ ($2.2 \times 10^{-14} \text{ cm}^3$) corresponding to an induced dipole moment of $7 \times 10^{-26} \text{ Cm}$ (2.1×10^4 Debye). Note that these numbers represent only estimates for the apparent values of the electric moments, because no reliable correction factors for the internal and the directing fields³² can be given at present. In any case, the bacteriorhodopsin molecules in purple membranes represent a highly polarizable system. In conclusion, the field strength dependence of the electro-optical data suggest that the orientational change of the chromophore is restricted both in extent and in direction. The unidirectional angular displacement of the chromophore is limited to $\Delta\theta_m = 0.35$ rad (20°) for $\omega=0$; the orientation direction is toward the membrane normal.

Cooperativity. One may note that the electric dipole moments of the orientation process, in particular the induced dipole moment, are

comparatively large. The permanent dipole moment may originate in the α -helices and in the paired polar groups (salt bridges) of bacteriorhodopsin. Since the seven α -helical segments are almost parallel to the membrane normal¹⁵, the dipole moment of one α -helix is not compensated by the oppositely directed moment of another α -helix. Furthermore, a segment contains on the average 30 ± 3 amino acid residues³³ and about 70% is α -helical³⁴. Because the dipole moment of one hydrogen bonded $\text{CO}\cdots\text{HN}$ group in an α -helix is 1.1×10^{-29} Cm (3.4 Debye)³⁵, the permanent dipole moment of these groups in one segment is about 2.3×10^{-28} Cm (69 Debye). Since the estimate of 4.7×10^{-28} from the experimental data is larger, either ionic side groups of the residues contribute appreciably to the electric moment, the orienting unit comprises more than one bacteriorhodopsin molecule, or the directing field is larger than the external field.

The primary sequence data³³ and x-ray crystallographic results¹⁵ suggest that the positively charged side groups of lysine and arginine residues and the negatively charged carboxylate side chains of aspartic and glutamic acid residues could form ion pairs of the type $\text{COO}^- \cdots \text{HN}^+$. Per bacteriorhodopsin, a maximum of 14 such pairs could be present. An applied field will shift the equilibrium $\text{COOH}\cdots\text{N} \rightleftharpoons \text{COO}^- + \text{HN}^+$ to the rhs.

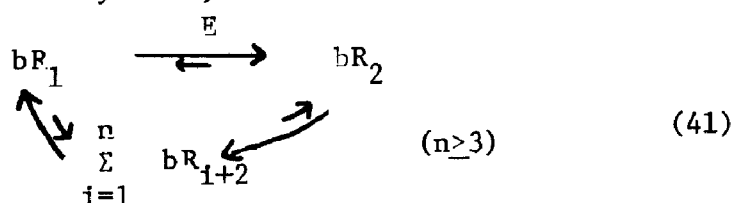
An induced dipole moment could now appear when the applied electric field increases the distance, ℓ , between the charged groups of an ion pair. In such a case the dipole moment changes from the zero-field value p_0 to a value $p_E = p_0 + \sum e_i \Delta \ell_i$ where e_i is the charge and $\Delta \ell_i$ is the field-dependent distance change in an ion pair of type i . The increase in ℓ_i then appears as an electric polarizability leading to an induced dipole moment.

If such an ion pair is formed at contact sites of different bacteriorhodopsin molecules in the membrane lattice, electrostatic coupling can be the origin of cooperative behavior. The magnitude of the measured induced dipole moment suggests that the orienting unit is not a single bacteriorhodopsin macromolecule, but rather represents a larger cluster of cooperatively coupled proteins.

Evidence for cooperativity in purple membranes is frequently reported. For instance, cooperativity is indicated in the binding of retinal to apomembranes³⁶, in the bleaching process³⁷, as well as in the proton-pump cycle¹¹. It has been suggested that cooperative units larger than the trimer are involved³⁶. If indeed larger clusters of bacteriorhodopsins orient the chromophores in a cooperative manner, then the electric axis of the orientation process is the vectorial sum of the various local contributions within the macromolecules. The local changes including the orientational displacement of the chromophore toward the membrane normal are the conformational transitions induced by the electric field, leading to a finite value of $A(\text{chem}) = \sum_i \epsilon_i \Delta c_i$. It is evident that the

conformational changes must involve at least one structure with a different extinction coefficient.

Reaction cycle. The enormous difference between the time ranges of the rise curve in the presence of the electric field and of the field-off response (see Figure 3) strongly suggests that the sequence of state changes caused by the electric field is different from the structural transitions occurring in the multi-state field off relaxation. The experimental data, therefore, suggest a cyclic reaction scheme which comprises at least five conformations in cooperative clusters of membrane-bound bacteriorhodopsin. The electric field causes a transition from state bR_1 to state bR_2 , whereas the field-off relaxation reflects the passage through at least three, probably more, intermediate conformations.



In the light of the orientation mechanism discussed above, the step $bR_1 \xrightarrow{E} bR_2$ may represent a 'synchronized', rapid alignment of ionic groups. These conformational changes appear to occur in the electric field in a concerted way and include a change in the chromophore transition moment from 1.2 rad (state bR_1) to the angle ≤ 0.87 rad (state bR_2).

We may now specify Eq. (19) in terms of these states by

$$\Delta A_{\sigma} = \{\Delta \epsilon_{1,\sigma}(1-x) + \Delta \epsilon_{2,\sigma}x\}c_T + (\bar{\epsilon}_2 - \bar{\epsilon}_1)xc_T \quad (42)$$

where $c_T = [bR_1] + [bR_2]$ is the total concentration of bacteriorhodopsin and $x = [bR_2]/c_T$ is the fraction in state bR_2 .

Since the experimental data indicate restricted angular displacement of the chromophore to only one direction, $x \leq 0.5$, at sufficiently high electric field where orientation is saturated, we have $x = 0.5$. For this case the extinction coefficient $\bar{\epsilon}_2$ is readily calculated from $\Delta A^{(chem)} = (\bar{\epsilon}_2 - \bar{\epsilon}_1)xc_T$. For instance, at 565 nm $\bar{\epsilon}_2 = 54000 \text{ M}^{-1}\text{cm}^{-1}$ and at 400 nm $\bar{\epsilon}_2 = 21000 \text{ M}^{-1}\text{cm}^{-1}$.

Although at the present accuracy of optical data recording the field-off relaxations appear to reflect at least four processes, the response curve is more probably a continuous spectrum of many local conformational transitions. Whereas the electric field acts simultaneously on all charged groups and dipoles of bacteriorhodopsin to cause a structural transition ($bR_1 \xrightarrow{E} bR_2$), the rearrangements in the absence of the field are more complex and face higher activation barriers, as is suggested by the larger relaxation times.

At present it is not possible to connect the 'electro-optic cycle' represented in scheme (41) with details of the photocycle. However, some aspects of field and light effects are worth mentioning. It has been recently observed that in dry films of purple membranes there are spectral similarities between the field-induced intermediates and the first intermediate of the photocycle [13].

The conformational changes evident by our electro-optic data clearly involve an orientational displacement of the chromophore toward the membrane normal. Interestingly, on the basis of Raman spectroscopic data it has been suggested that during the photocycle the chromophore rotates out of the membrane plane³⁸. A further correlation between the photocycle and the electro-optic data is the appearance of cooperativity.

Although the cyclic nature and the kinetics of the electric field induced structural changes suggest common features with the photocycle, further studies are necessary in order to identify the effect of electric field on the dynamic properties of bacteriorhodopsin.

The electric field effects observed in membrane-bound bacteriorhodopsin are, however, suggestive of a possibly general mechanism for a very effective interaction of electric fields with the ion flow gating proteins in excitable biomembranes [1-4]. The field dependence of the ion permeability changes underlying the nerve impulse and other membrane potential changes would then be molecularly based on a polarization mechanism where the distances between charged groups of the gating proteins depend on the intensity of the membrane electric field.

References

1. E. Neumann, in: Electro-optics and dielectrics of macromolecules and colloids, (Ed. B. R. Jennings) Plenum Press, New York, p. 233-245 (1979).
2. E. Neumann, in: Topics in Bioelectrochemistry and Bioenergetics, (Ed. G. Milazzo), John Wiley & Sons, London, Vol. 4, p. 113 - 161, (1980).
3. E. Neumann and J. Bernhardt, Ann. Rev. Biochem. 46, 117 (1977).
4. E. Neumann, Neurochemistry Intern. 1, in press (1980)
5. K. Tsuji and E. Neumann, Intern. J. Biol. Macromol. 2, in press, (1980).
6. D. Schallreuter and E. Neumann, in prep. (1980).
7. A. Revzin and E. Neumann, Biophys. Chem. 2, 144 (1974).
8. D. Oesterhelt and W. Stoeckenius, Nature New Biol. 233, 149 (1971).
9. D. Oesterhelt and W. Stoeckenius, Proc. Nat. Acad. Sci. USA, 70, 2853 (1973).
10. R. Shinar, S. Druckmann, M. Ottolenghi, and R. Korenstein, Biophys. J. 19, 1 (1977).
11. B. Hess, R. Korenstein, and D. Kuschmitz in 'Energetics and Structure of Halophilic Micro-organisms' (Eds. S. R. Caplan and M. Ginzburg), Elsevier, Amsterdam, p. 89 (1978).
12. K. Tsuji and K. Rosenheck in 'Electro-Optics and Dielectrics of Macromolecules and Colloids' (Ed. B. R. Jennings), Plenum Press, New York, p. 77, (1979).
13. G. P. Borisevitch, E. P. Lukashev, A. A. Kononenko and A. B. Rubin, Biochim. Biophys. Acta, 546, 171 (1979).
14. M. Eisenbach, C. Weissmann, G. Tanny, and S. R. Caplan, FEBS Lett. 81, 77 (1977).
15. R. Henderson, J. Mol. Biol. 93, 123 (1975).
16. A. N. Kriebel and A. C. Albrecht, J. Chem. Phys. 65, 4575, (1976).

17. T. G. Ebrey, B. Becher, B. Mao, P. Kilbride and B. Honig, J. Mol. Biol. 112, 377 (1977).
18. M. P. Heyn, R. J. Cherry and U. Müller, J. Mol. Biol. 117, 607, (1977).
19. C. T. O'Konski, K. Yoshioka and W. H. Orttung, J. Phys. Chem. 63, 1558 (1959).
20. E. Fredericq and C. Houssier, 'Electric Dichroism and Electric Birefringence', Clarendon Press, Oxford (1973).
21. F. J. Perrin, Phys. Radium, 7, 390 (1926).
22. A. E. Blaurock and W. Stoeckenius, Nature New Biol., 233, 152 (1971).
23. L. Keszthelyi, Biochim. Biophys. Acta, 598, 429 (1980).
24. K. Razi Naqvi, J. Gonzalez-Rodriguez, R. J. Cherry, and D. Chapman, Nature New Biol. 245, 249 (1973).
25. T. Konishi and L. Packer, FEBS Lett. 92, 1 (1978).
26. A. Lewis, M. A. Marcus, B. Ehrenberg, and H. Crespi, Proc. Nat. Acad. Sci. USA 75, 4642 (1978).
27. T. Gillbro, Biochim. Biophys. Acta 504, 175 (1978).
28. R. H. Lozier and W. Niederberger, Fed. Proc. 36, 1805 (1977).
29. K. Schulten and P. Tavan, Nature 272, 85 (1978).
30. J. B. Hurley, B. Becher, and T. G. Ebrey, Nature 272, 87 (1978).
31. K. Yoshioka and H. Watanabe in: 'Physical Principles and Techniques of Protein Chemistry, Part A' (Ed. S. J. Leach) Academic Press Inc., New York, p. 339 (1969).
32. C. J. F. Böttcher, 'Theory of Electric Polarization', Elsevier Sci. Pub. Co., Amsterdam (1973).
33. Yu. A. Ovchinnikov, N. G. Abdulaev, M. Yu Feigina, A. V. Kiselev and N. A. Lobanov, FEBS Lett. 100, 219 (1979).
34. B. Becher and J. Y. Cassim, Biophys. J. 16, 1183 (1976).
35. A. Wada in: 'Poly- α -Amino Acids' (Ed. G. Fasman), Marcel Dekker, New York, p. 369 (1967).

36. M. Rehorek and M. P. Heyn, Biochemistry, 18, 4977 (1979).
37. B. Becher and J. Y. Cassim, Biophys. J., 19, 285 (1977).
38. A. Lewis, Phil. Trans. R. Soc. Lond., A293, 315 (1979).